

A Note on Least-norm Solution of Global WireWarping

Charlie C. L. Wang

Department of Mechanical and Automation Engineering
The Chinese University of Hong Kong
Shatin, N.T., Hong Kong
E-mail: cwang@mae.cuhk.edu.hk

Abstract

WireWarping [1] is a fast surface flattening approach, which presents a very important property of length-preservation on feature curves. The global scheme of *WireWarping* formulates the warping problem into an optimization in angle space and solves it by using the Newton's method. However, some diverged examples were found in our recent tests. This technical note presents a least-norm solution in terms of angle-error for the global *WireWarping*. The experimental tests show that the least-norm solution is more robust than the Newton's algorithm.

1. Problem

The Newton's method solves a constrained optimization problem by converting the objective function and the constraints into an augmented objective function $J(X)$ with X as the variable vector. Then, the update vector δ in each iteration step is computed by the linear system, $\nabla^2 J(X)\delta = -\nabla J(X)$, which is formed by the Hessian matrix $\nabla^2 J(X)$ and the gradient $\nabla J(X)$. However, the Newton's algorithm has no control over the magnitude of δ . There, vibration is easily generated when the status variable X is near optimum. In some extreme cases, such vibration may move the system to a status that can hardly converge. Fig.1 shows such a vibrated example when using Newton's method to compute the global *WireWarping*.

To make the Newton's method more robust, the soft-line-search strategy [2] is always employed to determine the actual update step size $\alpha\delta$ ($0 < \alpha \leq 1$) (e.g., [3]). However, such a line-search introduces additional sub-routine of iterations so that actually slows down the computation. Stimulated by the recent work of least-norm solution of angle-based parameterization in [4], a least-norm solution is proposed in this note to increase the robustness of optimization while remaining the same efficiency as Newton's method in each iteration step.

The constrained optimization problem to be solved is Eq.(13) in [1].

$$\begin{aligned} & \min_{\theta_i} \sum_i (\theta_i - \alpha_i)^2 \\ s.t. \quad & n_p \pi - \sum_{b=1}^{n_p} \theta_{\Gamma_p(b)} \equiv 2\pi & (\forall p = 1, \dots, m) \\ & \sum_{b=1}^{n_p} l_b \cos \phi_b \equiv 0, \quad \sum_{b=1}^{n_p} l_b \sin \phi_b \equiv 0 & (\forall p = 1, \dots, m) \\ & \sum_{q_k \in v} \theta_k \equiv 2\pi & (\forall v \in \Phi) \end{aligned} \tag{1}$$

Here, we adopt the same nomenclature. Φ represents the collection of interior vertices on accessory feature curves, θ_i is the 2D angle associated with the wire-node q_i to be computed, α_i represents its optimal angle (i.e., the 3D angle employed in [1]), and l_b denotes the length of an edge on wires. To simplify the expression, a permutation function $\Gamma_p(b)$ is used to return the global index of a wire-node on the wire patch P_p with the local index b , and its inverse function $\Gamma_p^{-1}(j)$ that gives the local index of a wire-node q_j on the wire-patch P_p .

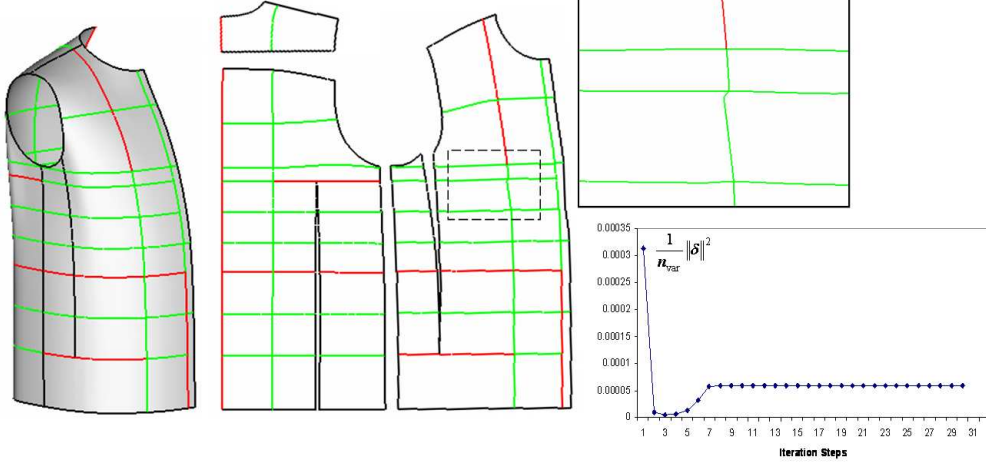


Figure 1: Numerical vibration occurs when using the global *WireWarping* to flatten the front piece of a shirt – as shown in the zoom-window, unwanted curve distortion is generated. This is because that the numerical computation vibrates – see the chart of $\|\delta\|^2$. Here, green and red lines represent the key feature curves and the accessory feature curves following [1].

2. Least-norm Solution

As stated in [4], carefully selecting alternative variables could make the linearization more accurate so that the computation converges faster than the Newton steps. We reformulate Eq.(1) by changing the variables from θ_i to the angle estimation error $e_i = \theta_i - \beta_i$, where β_i is the current angle at wire-node i and θ_i is the optimal angle to be computed. The optimization problem in Eq.(1) is reformulated as

$$\begin{aligned}
 & \min_{e_i} \sum_i e_i^2 \\
 \text{s.t. } & n_p \pi - \sum_{b=1}^{n_p} (\beta_{\Gamma_p(b)} + e_{\Gamma_p(b)}) \equiv 2\pi \quad (\forall p = 1, \dots, m) \\
 & \sum_{b=1}^{n_p} l_b \cos \phi_b \equiv 0, \quad \sum_{b=1}^{n_p} l_b \sin \phi_b \equiv 0 \quad (\forall p = 1, \dots, m) \\
 & \sum_{q_k \in v} (\beta_k + e_k) \equiv 2\pi \quad (\forall v \in \Phi)
 \end{aligned} \tag{2}$$

For the constraints with ϕ_b , as $\phi_i = \pi - (e_i + \beta_i) + \phi_{i-1}$ and $\phi_1 = \pi - (e_1 + \beta_1)$ according to Eq.(3) in [1], ϕ_i can be expressed as

$$\phi_i = i\pi - \sum_{h=1}^i (e_h + \beta_h) = \Delta_i + \xi_i$$

with $\Delta_i = i\pi - \sum_{h=1}^i \beta_h$ and $\xi_i = -\sum_{h=1}^i e_h$. Using Taylor expansion

$$\begin{aligned}
 \cos(\Delta_i + \xi_i) &= \cos \Delta_i + (-\sin \Delta_i)\xi_i + (-\frac{1}{2} \cos \Delta_i)\xi_i^2 + \dots \\
 \sin(\Delta_i + \xi_i) &= \sin \Delta_i + (\cos \Delta_i)\xi_i + (-\frac{1}{2} \sin \Delta_i)\xi_i^2 + \dots
 \end{aligned}$$

we then truncate the series by retaining the linear terms only (i.e., with the approximation error $O(\xi_i^2)$). Therefore, the non-linear constraints $\sum_{b=1}^{n_p} l_b \cos \phi_b \equiv 0$ and $\sum_{b=1}^{n_p} l_b \sin \phi_b \equiv 0$ are linearized into

$$\sum_{b=1}^{n_p} (e_{\Gamma_p(b)} \sum_{i=b}^{n_p} l_i \sin \Delta_i) = -\sum_{i=1}^{n_p} l_i \cos \Delta_i \tag{3}$$

and

$$\sum_{b=1}^{n_p} (e_{\Gamma_p(b)} \sum_{i=b}^{n_p} l_i \cos \Delta_i) = \sum_{i=1}^{n_p} l_i \sin \Delta_i \tag{4}$$

respectively. In summary, Eq.(2) is converted into

$$\min \|\mathbf{r}\|^2 \text{ s.t. } \mathbf{C}\mathbf{r} = \mathbf{b} \quad (5)$$

where \mathbf{C} is a $n_{con} \times n_{var}$ matrix. As discussed in [1], if there are l wire-nodes with their 2D angles locked by the key feature curves, the number of variables for the above problem is $n_{var} = (\sum_{p=1}^m n_p) - l$. If there are r interior vertices on the accessory feature curves, the total number of constraints is $n_{con} = 3m + r$.

In general, $n_{con} < n_{var}$, there are multiple solutions for $\mathbf{C}\mathbf{r} = \mathbf{b}$. Among them, we need to seek one that leads to a minimal norm $\|\mathbf{r}\|^2$ on the variable vector \mathbf{r} . This is a least-norm problem. For a full rank coefficient matrix \mathbf{C} , the least-norm problem has a unique solution (c.f. [5])

$$\mathbf{r} = \mathbf{C}^T(\mathbf{C}\mathbf{C}^T)^{-1}\mathbf{b} \quad (6)$$

The value of \mathbf{r} can be solved by finding a solution to the normal equation $(\mathbf{C}\mathbf{C}^T)\mathbf{x} = \mathbf{b}$ following by a substitution that $\mathbf{r} = \mathbf{C}^T\mathbf{x}$. The matrix \mathbf{C} has full rank as the constraints in Eq.(1) are independent.

Starting from letting $\beta_i = \beta_i^0$, we iteratively update the value of β_i by solving e_i in Eq.(5) and update its value with $\beta_i = \beta_i + e_i$ in each step. The iteration is stopped when $\frac{1}{n_{var}}\|\mathbf{r}\|^2 < 10^{-8}$ is satisfied. The resultant optimal angle for each wire-node is then determined. Why such a least-norm solution in each iteration step is more robust? The major reason is that among all possible solutions, the one with minimal estimation error is adopted. While the Newton's update just move the system variables along the optimal direction but not determine an optimal step size when not conducting the soft-line-search strategy, the least-norm solution actually mimics the soft-line-search. Another minor benefit of the least-norm solution is that we do not need to compute the second derivative of $J(X)$.

Although the case of $n_{con} \geq n_{var}$ is never found in our tests, the linearization of global warping problem as Eq.(2-4) gives a possible solution to compute the update vector \mathbf{r} by

$$\mathbf{C}^T\mathbf{C}\mathbf{r} = \mathbf{C}^T\mathbf{b} \quad (7)$$

which is in fact a least-square solution.

3. Initial Value

Same other optimization techniques, the least-norm solution still relies on good initial angle values on wire-nodes. In the original publication [1], 3D angles are employed to be the initial angle values on wire-nodes. However, this does not give satisfactory results when flattening some highly curved surfaces (e.g., the pants of wet-suit in Fig.2 which are also shown in [1]).

For those surfaces without key feature curves determined (e.g., Fig.2), the warping of feature curves are flexible. Thus, the Least-Square Conformal Map presented in [6] is used to pre-flatten the surface into plane, and the 2D angle at each wire-node is then adopted as the initial value of iteration. For those surfaces with the shape of key feature curves specified (e.g., the perpendicular key feature curves are specified in Fig.1), the initial value β_i^0 at a wire-node q_i is determined as

$$\beta_i^0 = \begin{cases} \alpha_i(2\pi - \sum_{q_j \in v} \alpha_j^L) / \sum_{q_k \in v} \alpha_k & q_i \in v, v \in \Phi \\ \alpha_i & otherwise \end{cases} \quad (8)$$

where q_k and q_j are the wire-node associated with the same vertex as q_i . q_j is the node on key feature curves with its 2D angle specified as α_j^L , q_k is on an accessory feature curve, and Φ is the set of interior vertices on accessory feature curves.

The initial value of angles determined by the above methods ensure that the angle compatible constraint $-\sum_{q_k \in v} \theta_k \equiv 2\pi$ ($\forall v \in \Phi$) has been satisfied at the beginning, which makes the computation easier to converge.

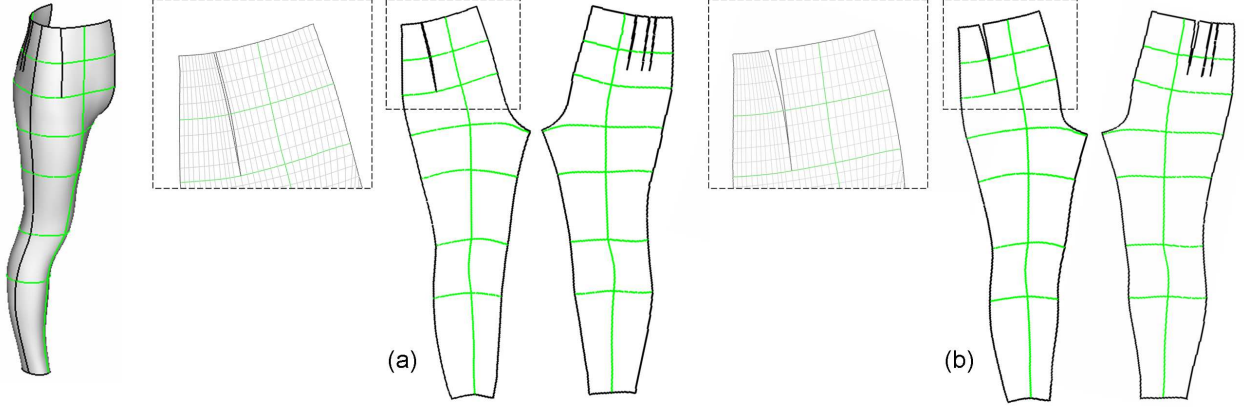


Figure 2: Different initial values will lead to different results: (a) with 3D angles as initial values – unwanted overlapping is generated at the darts, and (b) using the result of least-square conformal map [6] as initial values – the result has been improved. Both results are generated by the least-norm solution of global warping.

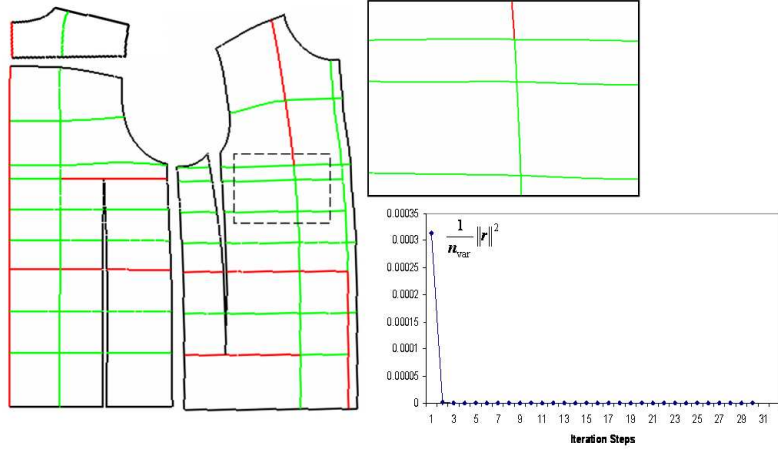


Figure 3: The flattening result by the least-norm solution of global WireWarping – the initial value is computed by Eq.(8).

4. Experimental Results

The least-norm solution of the global *WireWarping* introduced in this technical note has been tested on several examples. The first test is given to the shirt model shown in Fig.1. The result by using the least-norm solution is given in Fig.3, and it is easy to find that the computation converges very fast (i.e., $\frac{1}{n_{var}} \|\mathbf{r}\|^2 \rightarrow 0$ after two steps of iteration). A more fair comparison is given on the norm of residual vector σ of the constrain equations in Eq.(1). More specifically, the residual vector is

$$\sigma = \begin{bmatrix} (n_p - 2)\pi - \sum_{b=1}^{n_p} \theta_{\Gamma_p(b)} \\ \sum_{b=1}^{n_p} l_b \cos \phi_b \\ \sum_{b=1}^{n_p} l_b \sin \phi_b \\ 2\pi - \sum_{q_k \in v} \theta_k \end{bmatrix}. \quad (9)$$

Figure 4 and 5 show the comparison, which is consistent with the norm of update vector – i.e., the least-norm solution converges faster and is also with less vibration.

The least-norm solution solves a linear equation system with dimension $n_{con} \times n_{con}$ (i.e., \mathbf{CC}^T)

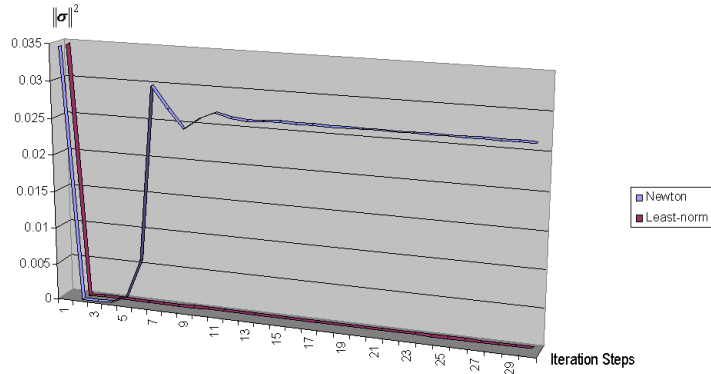


Figure 4: Chart for comparing the convergency on the norm of residual vector by the Newton’s method vs. the least-norm solution.

in each iteration plus one step of substitution. For the numerical computation proposed in [1], in Eq.(23)-(24), the update vector in each step is also determined by computing a $(3m + r) \times (3m + r)$ linear system followed by substitution. As $n_{con} = 3m + r$, the computations in each step by the method of [1] and the least-norm solution are the same. Therefore, the computation speed of least-norm solution is faster as it usually needs less steps than Newton’s method does to converge.

Acknowledgments

The author would like to thank TPC (HK) Ltd for providing the 3D surface patches of garment suits.

References

- [1] C.C.L. Wang, "WireWarping: A fast surface flattening approach with length-preserved feature curves", *Computer-Aided Design*, vol.40, no.3, pp.381-395, 2008.
- [2] K. Madsen, H.B. Nielsen, and O. Tingleff, *Optimization with Constraints*, Lecture Notes, 2004.
- [3] Y. Liu, H. Pottmann, J. Wallner, Y.-L. Yang, and W. Wang, "Geometric modeling with conical meshes and developable surfaces", *ACM Transactions on Graphics*, vol.25, no.3, pp.681-689, 2006.
- [4] R. Zayer, B. Lévy, and H.-P. Seidel, "Linear angle based parameterization", *Proceedings of Eurographics Symposium on Geometry Processing*, 2007.
- [5] L. Vandenberghe, *Applied Numerical Computing*, Lecture Notes, 2007.
- [6] B. Lévy, S. Petitjean, N. Ray, and J. Maillot, "Least squares conformal maps for automatic texture atlas generation", *ACM Transactions on Graphics*, vol.21, no.3, pp.362-371, 2002.

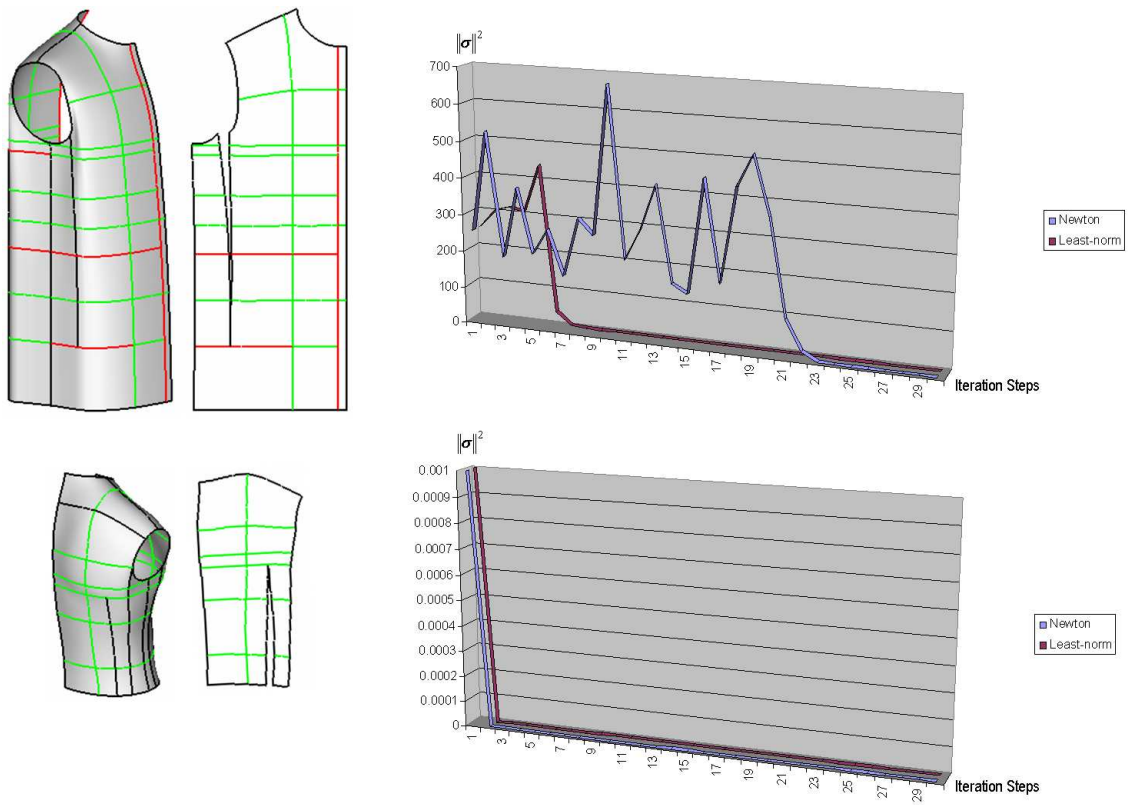


Figure 5: Another example for comparing the convergency on the norm of residual vector by the Newton's method vs. the least-norm solution.